# Inhomogeneous Light Shifts of Coherent Population Trapping Resonances

J. W. Pollock,[1,2] V. I. Yudin,[3,4,5] A. V. Taichenachev,[3,4] M. Yu. Basalaev,[3,4,5] D. V. Kovalenko,[3,4] A. Hansen,[1,6] J. Kitching,[1,2] and W. R. McGehee[1,a)]

[1)] *National Institute of Standards and Technology, Boulder, Colorado 80305, USA*

[2)] *Department of Physics, University of Colorado, Boulder, Colorado 80309, USA*

[3)] *Novosibirsk State University, ul. Pirogova 1, Novosibirsk, 630090, Russia*

[4)] *Institute of Laser Physics SB RAS, pr. Akademika Lavrent'eva 3, Novosibirsk, 630090, Russia*

[5)] *Novosibirsk State Technical University, pr. Karla Marksa 20, Novosibirsk, 630073, Russia*

[6)] *Present address: Quantinuum, 303 S. Technology Ct., Broomfield, Colorado 80021 USA*

(Dated: 22 August 2022)

Coherent population trapping (CPT) in atomic vapors using all-optical interrogation has enabled the miniaturization of microwave atomic clocks. Light shifts induced by the CPT driving fields can impact the spectral profile of CPT resonances and are a common limit to the long-term stability of CPT clocks. Nonlinear light shifts have been observed in several CPT systems and have not been explored in detail. In this Letter, we demonstrate that nonlinear light shifts in CPT clocks can arise from spatially-inhomogeneous CPT driving fields. We measure this effect using Gaussian laser beams in a buffer gas cell and show strong agreement with a four-level model describing the CPT Λ-system with a noninteracting "trap" state. We estimate the effect of this nonlinearity on recently-developed light shift mitigation techniques and suggest improvements to existing techniques.

The development of atomic clocks has led to numerous advances in science and technology: global navigation satellite systems, high-speed telecommunications, secure-data transfer, relativistic geodesy, verification of fundamental physical theories, and more.[1–9] Microwave atomic clocks using a vapor cell have been developed for applications where small size, low-power consumption, simplicity, and reliability of the design are important. In particular, atomic clocks based on coherent population trapping (CPT)[10–14] have great potential as all-optical interrogation allows for miniaturization in the absence of a microwave resonator[15–17] and overall simplification of the clock architecture.

A major limitation to the stability of CPT atomic clocks is the light (ac Stark) shift that arises from the interaction of atoms with the driving laser fields. Light shifts are present in both continuous-wave[18–23] (CW) and pulsed[20,23–29] schemes. Multiple methods for suppressing the effect of light-field-parameter fluctuations on the stabilized clock frequency have been developed for CW[18,19,30–33] and pulsed[34–41] CPT interrogation. Recent CW power-modulation (PM) schemes mitigate light shifts using measurements at two alternating interrogation laser powers[42] and have demonstrated a five-fold improvement in the long-term stability.[43] However, these PM schemes[42,43] are most effective for light shifts that scale linearly with the laser power. Nonlinear light shifts[18,23,43–47] lead to residual frequency instability in CW CPT systems, but the origins of these nonlinear shifts have not been explored in detail.

Previous studies using spatially-inhomogeneous interrogating fields have demonstrated modified three-level resonance shapes.[48–53] CPT resonances measured in buffer gas cells, which limit the effective interaction volume of Rb atoms with the driving fields, display "sharply-peaked" lineshapes with sub-Lorentzian widths when interrogated with Gaussian-profile fields.[50,52] Intermittent interaction with CW CPT fields arising from diffusive motion in buffer gas cells generates similarly peaked resonances.[54–56] The interrogating beam profile is known to impact the observed lineshapes in double-resonance microwave atomic clocks and leads to nonlinear light shifts when the transitions are inhomogeneously broadened.[48]

In this Letter, we demonstrate that nonlinear light shifts can arise in CPT clocks using spatially-inhomogeneous driving fields. Our work centers on Rb atoms in a buffer gas cell interrogated using Gaussian-profiled laser beams. Collisions with the buffer gas atoms limit the effective interaction volume of Rb atoms with the driving fields, with this volume determined by the atom's mean free path within a CPT coherence time. We explore the limit in which atoms are effectively immobile, or "stuck" in the buffer gas, and form spatially-varying equilibrium resonances set by the local properties of the driving fields.[48,52] In this limit, spatially-varying resonance contrast, broadening, and light shifts lead to a nonlinear shift of the CPT resonances measured using the global transmission of the interrogating beam through the buffer gas cell (Fig. 1(a)). We measure the spectral properties of CPT resonances using Gaussian-profiled beams and compare the results to measurements made using approximately single-intensity, flattop beams. Measurements are described using a four-level model including the CPT Λ-system with a noninteract-

[a)] Author to whom correspondence should be addressed: william.mcgehee@nist.gov

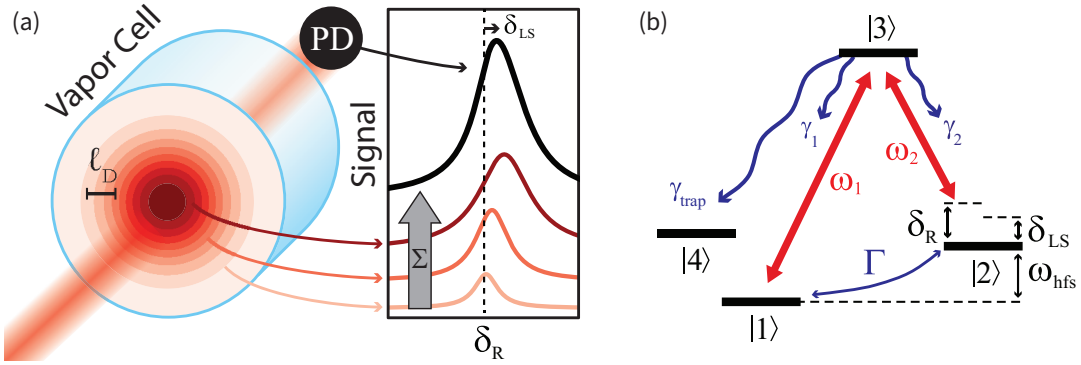


FIG. 1. Schematic of CPT resonances in the stuck-in-the-buffer-gas limit. (a) Rb atoms in a buffer gas cell are interrogated using a Gaussian laser beam. For typical buffer gas pressures, the distance atoms diffuse in a coherence time ($\ell_D$) is smaller than the spatial structure of the interrogating beam. In this limit, atoms form equilibrium resonances with their local environment (colored lines), leading to variation in resonance contrast, broadening, and lights shifts across the cell. Integrated CPT resonance (black line) measured using a photodiode (PD) is a sum of the spatially-inhomogeneous resonances in the cell. (b) The CPT resonances formed between states $|1\rangle$ and $|2\rangle$ are well described by a four-level model including the CPT $\Lambda$-system with a noninteracting trap state. Here, $\omega_1$ and $\omega_2$ label the interrogating fields; $\gamma$-terms represent relaxation from $|3\rangle$; $\Gamma$ represents the total decoherence rate of the CPT state involving $|1\rangle$ and $|2\rangle$; $\delta$-terms represent frequency detunings.

ing trap state.[13,57]

The CPT $\Lambda$-system is formed using the $5S_{1/2}, F$=1,2 $\leftrightarrow$ $5P_{1/2}$, F'=2 (D1) transitions in $^{87}$Rb, shown schematically in Fig 1(b). Light is generated using a distributed Bragg reflector laser and phase modulated near the Rb ground state hyperfine transition frequency $\omega_{\rm hfs}$ ($\approx$ 6.834 GHz) using a fiber-coupled electro-optic modulator. The carrier and +1 sideband address the CPT-$\Lambda$ system with approximately equal powers (modulation index $\approx$ 1.4). The light is circularly polarized and shaped to form a collimated Gaussian beam with a $\approx$ 2.4 mm $1/e^2$ radius before it passes through the buffer gas cell.

Measurements are made using a cylindrical cell filled with $^{87}$Rb and a $\approx$ 6.5 kPa buffer gas mixture of Ar and $N_2$ gas ($\approx$ 6:1 ratio). The cell has a nominal 1 cm radius and 2.8 cm length and is temperature stabilized near 303 K such that $\approx$ 10 % of the interrogating field is absorbed on the Doppler-broadened Rb one-photon resonances. A $\approx$ 3.6 $\mu$T spin quantization magnetic field is applied along the laser propagation axis. The cell is considered optically thin, and intensity variation within the cell is dominated by the transverse Gaussian profile of the CPT light. At this buffer gas pressure, the ground state relaxation rate from buffer gas collisions is estimated to be $\approx 2\pi \times 50$ Hz and is the dominant contribution to the total ground state relaxation rate $\Gamma$ in our system.[17,58]

The stuck-in-the-buffer-gas condition we explore is satisfied when the coherence limited, 1D-diffusion length is less than the size of the beam. We define this diffusion length $\ell_D = \sqrt{2D/\Gamma}$, where the diffusion constant $D \approx 2.3$ cm$^2$ s$^{-1}$ for the buffer mixture and pressure in our cell results in $\ell_D \approx 1.1$ mm. This satisfies the stuck-in-the-buffer-gas condition for our beam geometry (Fig. 1(a)). The buffer gas pressure in CPT vapor cell clocks is often optimized to balance relaxation rates from wall and buffer gas collisions, setting the scale of the highest-order relevant diffusion mode at approximately the size of the cell.[17] This implies that the stuck-in-the-buffer-gas condition is at least partially satisfied in many CPT clocks.

To model the atomic medium, we consider a four-level system (Fig. 1(b)) interacting with a bichromatic electric field $E(t) = E_1 e^{-i\omega_1 t} + E_2 e^{-i\omega_2 t}$ + c.c.. This model corresponds, for example, to the $\Lambda$-system formed when addressing the two ground hyperfine, $m_F = 0$ states of Rb using the $D_1$ line. We include a trap state (e.g. an extreme Zeeman sublevel of the ground state) where significant population can accumulate due to optical pumping.[57] The trap state population no longer interacts with the driving fields and does not contribute to the CPT resonance. The CPT resonance occurs near zero two-photon detuning $\delta_R = \omega_1 - \omega_2 - \omega_{\rm hfs}$, where $\omega_{\rm hfs}$ corresponds to the transition frequency between the hyperfine ground states of the $\Lambda$-system including buffer gas shifts. Under this condition, atomic population is optically pumped into a coherent superposition of the ground states, and absorption in the cell is reduced.

The temporal dynamics of the quantum system can be described using the formalism of the atomic density matrix $\hat{\rho}(t)$. The optical power absorbed through an optically-thin cell is proportional to the excited-state population $\rho_{33}$ as absorption arises due to spontaneous decay of the excited state. The steady-state solution for $\rho_{33}$ (see SM for details) is a symmetrical Lorentzian resonance. Near zero one-photon detuning and with equal driving field amplitudes, the resonance absorption contrast is

$$c_A(\delta_{\rm R}) = K \frac{W}{1+qW} \frac{\gamma_{\rm d}^2}{\gamma_{\rm d}^2 + (\delta_{\rm R} - \delta_{\rm LS})^2}, \qquad (1)$$

where $K$ is a numerical factor describing the magnitude of the response, $W = (\Omega_1^2 + \Omega_2^2)/\Gamma\gamma_{\rm opt}$ characterizes the strength of the interrogating field, $q = 1+\gamma_{\rm trap}/\gamma_{\rm sp}$ represents the openness of the $\Lambda$-system, $\delta_{\rm LS}$ is the light shift, and

$$\gamma_{\rm d} = \Gamma(1+W)\sqrt{\frac{1+qW}{1+qW+(q-1)W^2}} \qquad (2)$$

is the half width at half maximum (HWHM) of the resonance. We define the parameters $\Omega_1 = d_{31}E_1/\hbar$ and $\Omega_2 = d_{32}E_2/\hbar$ as the Rabi frequencies for transitions $|1\rangle \leftrightarrow |3\rangle$ and $|2\rangle \leftrightarrow |3\rangle$, respectively ($d_{31}$ and $d_{32}$ are the matrix elements of the operator of electrical dipole moment); $\gamma_{\rm opt}$ is the decay rate of optical coherence; $\gamma_{\rm trap}$ is the rate of spontaneous population transfer from a state $|3\rangle$ to trap state $|4\rangle$; $\gamma_{\rm sp} = \gamma_1 + \gamma_2 + \gamma_{\rm trap}$ is the total spontaneous decay rate of the excited state $|3\rangle$, where $\gamma_1$ and $\gamma_2$ are the rates of spontaneous population transfer from a state $|3\rangle$ to states $|1\rangle$ and $|2\rangle$, respectively and are assumed to be equal; and $\Gamma$ is the ground-state relaxation rate in the absence of the light.

We demonstrate the utility of the four-level model through comparison to CPT resonances measured at single-field intensities. This "single-intensity" configuration is achieved by measuring only the central portion of the Gaussian beam using an aperture placed in the beam after it passes through the buffer gas cell. The aperture is centered on the CPT beam with an approximate 1 mm diameter, and the average intensity in the apodized beam is $I_{avg} \approx 94$ % of the Gaussian peak intensity $I_{\rm peak}$. The transmitted optical power is measured using a photodiode. CPT spectra (Fig. 2(a)) are acquired in this configuration for varying $I_{\rm peak}$ with absorption contrast values observed up to $\approx 12$ %. The spectra have an approximately Lorentzian profile with deviations from this profile observed at less than 1 % in the peak absorption contrast magnitude (see SM). We attribute these relatively small deviations from a Lorentzian spectrum to diffusion-induced Ramsey narrowing arising from the repeated, intermittent interaction with the beam.[54–56]

Broadening and contrast of the single-intensity CPT resonance are numerically extracted from the spectral profiles and plotted in Fig. 2(c,d). The observed trends are consistent with Eqs. 1 and 2; using this model and $W = \alpha I_{\rm peak}$, we find that $\Gamma = 2\pi \times (50 \pm 5)$ Hz, $\alpha = 0.8 \pm 0.2$ m$^2$/W, $q = 1.05 \pm 0.04$, and $K = 0.159 \pm 0.002$. Here, error bars are one standard deviation intervals for fitted values. The value for $\Gamma$ agrees with expected numerical values set by the collisional broadening.[17,58] Evidence of the trap state is demonstrated in the nonlinear broadening of the CPT resonance in Fig. 2(c) compared to the linear broadening typical to closed-$\Lambda$ systems (Eq. 2 with $q = 1$).

To demonstrate the impact of the Gaussian-intensity profile on the CPT resonance, spectra were acquired using the full interrogating beam (no aperture) as shown in Fig. 2(b). In the stuck-in-the-buffer-gas limit, the composite resonances formed by integrating over the cylindrically-symmetric spatial profile of the CPT fields is a sum of Lorentzian resonances with widths, shifts, and amplitudes determined by the local intensity[52] (Fig. 1(b)) as

$$\langle\rho_{33}\rangle_{\delta_{\rm R}} = 2\pi\int_0^\infty r\left(B(r) + \frac{A(r)\gamma_{\rm d}^2(r)}{\left[\delta_{\rm R} - \delta_{\rm LS}(r)\right]^2 + \gamma_{\rm d}^2(r)}\right)dr. \qquad (3)$$

Here, $B(r)$ and $A(r)$ are the local magnitudes of the one-photon and two-photon absorption (see SM), respectively, and the angled brackets indicate spatial averaging. The HWHM and $c_A$ are again numerically extracted from the spectra and plotted in Fig. 2(c,d). The shape of the measured "Gaussian-averaged" resonances remains largely Lorentzian with a subtle asymmetry due to the light shift. Analytical expressions for the CPT resonance integrated over a Gaussian profile can be found for a closed $\Lambda$-system ($q = 1$) with[59] and without[52] the light shift term. We numerically integrate Eq. 3 in this work to account for the light shift and $q$-dependent effects.

The width and absorption contrast of the Gaussian-averaged data can be closely reproduced with no free parameters using Eq. 3 and the single-intensity values for $\Gamma$, $\alpha$, $q$, and $K$ as shown in Fig. 2(c-d). In this comparison, deviation from the model is observed at the 10 % level, likely arising from diffusive effects including Ramsey narrowing.[54–56]

While evidence of the light shift is present in the spectral data, determination of the shift values at varying $I_{\rm peak}$ is achieved with greater accuracy by stabilizing the oscillator driving the CPT resonance using the atomic response. Here, locking of the resonator is achieved using square-wave frequency modulation to form an error signal

$$S_{\rm err}(\delta_{\rm R}) \propto \langle\rho_{33}\rangle_{\delta_{\rm R}+\delta_{\rm J}/2} - \langle\rho_{33}\rangle_{\delta_{\rm R}-\delta_{\rm J}/2}, \qquad (4)$$

where $\delta_J$ is the magnitude of the frequency modulation. Data are acquired in both the single-intensity and the Gaussian-averaged configurations (Fig. 3) using a frequency jump $\delta_J = 200$ Hz. We stabilize the oscillator using $S_{err}$ and define the frequency shift $\delta_{err}$ relative to $\omega_{hfs}$, which includes a collisional shift of

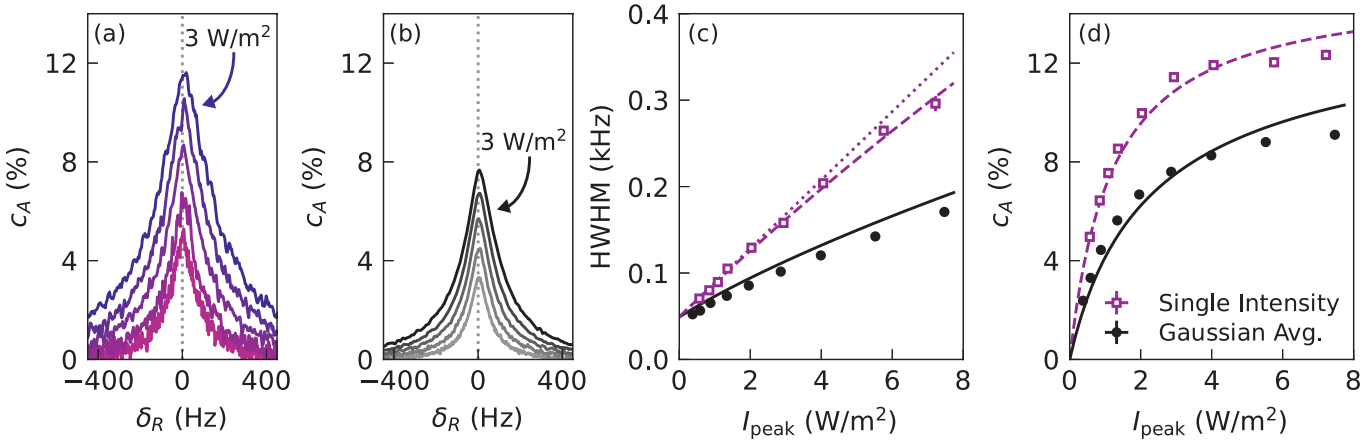


FIG. 2. Broadening and contrast of CPT spectra. Measured single-intensity (a) and Gaussian-averaged (b) CPT spectra are plotted for approximate peak intensities of 0.6 W/m$^2$, 0.8 W/m$^2$, 1.3 W/m$^2$, 2 W/m$^2$, and 3 W/m$^2$ (increasing from light to dark). The signal-to-noise ratio is lower for the single-intensity data due to the lower optical powers detected. Lorentzian fitting to measured spectra is used to extract the HWHM (c) and peak absorption contrast (d) as $I_{\mathrm{peak}}$ is varied in both the single intensity (open purple squares) and Gaussian-averaged (filled black circles) configurations. The single-intensity data in (c,d) are fitted to Eqs. 1 and 2 (dashed purple lines in c,d) to extract $\alpha$, $\Gamma$, and $q$ in the four-level model. Comparison of the Gaussian-averaged data is made to Eq. 3 (solid black lines in c,d) using the extracted single-intensity values with no free parameters. The HWHM expected for a closed system (Eq. 2, $q = 1$) is plotted (c, dotted purple line) for comparison. Error bars in (c,d) are one standard deviation confidence intervals, and some error bars are smaller than the points.

$2\pi \times (-1303.1 \pm 0.2)$ Hz. The single-intensity light shift data are plotted in Fig. 3 and demonstrate a linear shift of the error signal $\delta_{err} = \xi I_{\mathrm{peak}}$ that arises from the light shift induced by the various frequency components of the phase-modulated light interacting with the energy-level structure of Rb (including levels and fields not pictured in Fig. 1(b)).[18,22,29] Best fit parameters for $\xi = 2\pi \times (3.4 \pm .1)$ Hz/(W/m$^2$).

Light-shift values in the Gaussian-averaged configuration (Fig. 3) show sub-linear growth as $I_{\mathrm{peak}}$ is varied. Comparison to the predicted shifts from Eqs. 3-4 is made using values for $\Gamma$, $\alpha$, $q$ and $\xi$ extracted from the single-intensity data. Strong agreement with the model is observed with no free parameters, which is consistent with the stuck-in-the-buffer-gas model of local shifts contributing to a composite, asymmetrical resonance. The discrepancy between Gaussian-averaged shifts and theory at low intensity could arise from diffusion-induced effects or less strongly satisfying the stuck-in-the-buffer-gas assumption. Frequency offsets arising from thermal buffer gas shifts limit systematic comparison of the data sets in Fig. 3 to $\pm 0.3$ Hz (68 % confidence interval).

The nonlinear light shift observed in the Gaussian-averaged configuration arises from a power-dependent asymmetry of the CPT resonance due to the spatial variation of the driving field. Other sources of asymmetry exist in CPT clocks including inhomogeneous magnetic fields, temperature gradients, and effects from one-photon detuning and imbalanced CPT fields.[60,61] We measure magnetic field variation in the probed volume to be less than $\approx 0.4$ $\mu$T using a magnetically-sensitive CPT resonance, placing an upper bound on $\approx 0.2$ Hz for the variation in Zeeman shift of the clock state. In our experiment, the powers in the CPT fields are set to be equal and the detuning from one-photon resonance is $\approx 0.5\gamma_{\mathrm{opt}}$. These effects are not expected to lead to significant nonlinearity of the single-intensity light shifts and none was observed (Fig. 3). Occupation of the trap state also impacts the Gaussian-averaged light shift due to spatial variation in the single-intensity absorption contrast and HWHM (Fig. 2(c,d)). The expected difference in $\delta_{err}$ between $q = 1.05$ and $q = 1$ calculated using Eq. 4 and the single-intensity values for $\Gamma$, $\alpha$, and $\xi$ is $\approx$ 0.1 Hz at $I_{\mathrm{peak}} = 8$ W/m$^2$. This trap state induced shift is significantly smaller than the observed non-linearity in the Gaussian-averaged data.

Nonlinear light shifts limit the effectiveness of recent PM techniques used to extrapolate the measured error signals to a light-shift-free value. For the nonlinear shift observed in the Gaussian-averaged data (Fig. 3), we calculate the frequency shift that would be measured using the linear PM scheme[42,43] and measurements made at $I_{\mathrm{peak}}$ and $I_{\mathrm{peak}}/2$. Under these assumptions, the sensitivity to light shifts (slope of the shift vs. $I_{\mathrm{peak}}$; details in SM) is reduced by a factor of $\approx 6$ at $I_{\mathrm{peak}} = 2$ W/m$^2$, similar to the improvement observed in Ref. 43.

Improvements to light-shift suppression techniques, including PM schemes,[42,43] are likely needed to achieve greater suppression of light shifts in CPT clocks. Aside from attempts to linearize the shift using homogeneous driving fields, methods can be adapted to include nonlinear terms which better reproduce known dependence on the light shift.[43] Additionally, modeling using Eq. 3 and Eq. 4 shows that the nonlinearity of the shift depends on the strength of the trap state $q$ and the magnitude of the frequency-jump modulation $\delta_J$. The non-

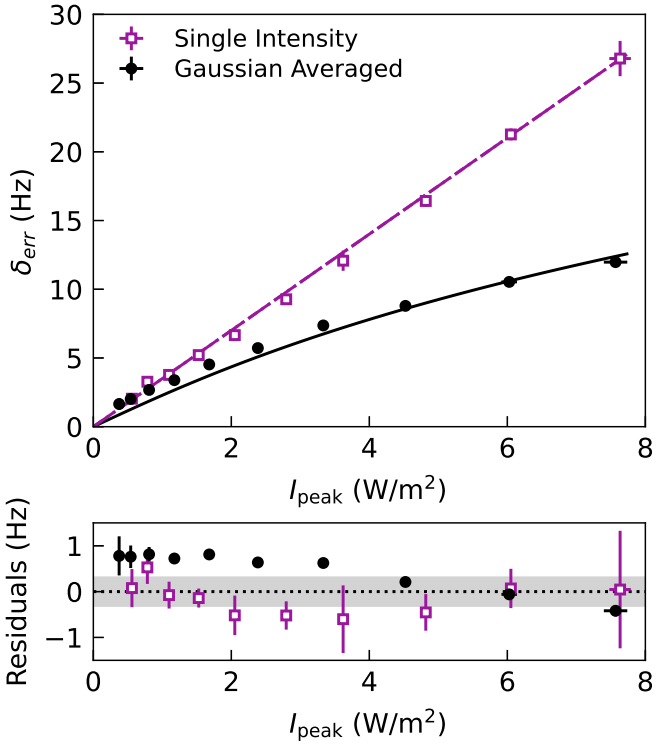


FIG. 3. Light shifts of the CPT resonance in the single-intensity (open purple squares) and Gaussian-averaged (filled black circles) configurations. (top) The single-intensity data demonstrate linear shifts (dashed purple line) while the Gaussian-averaged data demonstrate nonlinear shifts consistent with the numerically calculated values using the measured single-intensity parameters and no free parameters (solid black line). (bottom) Residuals are shown for the theoretical comparisons. Error bars are the overlapping Allan deviation at 1 s; some error bars are smaller than the points. The grey band indicates the systematic uncertainty between the Gaussian-averaged and single-intensity data sets due to thermal drift.

linearity of the shift can be reduced with increased $\delta_J$ by interrogating the power-broadened wings of the CPT resonance that are primarily set by atoms near the center of the Gaussian profile. Operating with a larger $\delta_J$ will likely restore the effectiveness of PM schemes at the cost of reduced short-term stability. Alternatively, spatially resolving the variation of the light shift across the CPT beams in the stuck-in-the-buffer-gas limit may enable light-shift-free frequency extrapolation without the use of time-varying laser power modulation.

In this work, we have explored light shifts in CPT clocks where atoms are effectively immobile in the buffer gas and form equilibrium resonances controlled by their local environment. We have measured the spectral properties in this limit for both single-intensity interrogation as well as signals acquired averaging over a Gaussian intensity profile. The data has been well described using a four-level model including the CPT Λ-system and a non-interacting trap state. We have reproduced the Gaussian-averaged behavior using this model with only measured, single-intensity parameters and no free parameters. Light shifts have been measured in both experimental configurations, and spatially-inhomogeneous driving fields are shown to cause nonlinear light shifts with optical power. These nonlinear light shifts limit the effectiveness of some common light-shift suppression schemes,[42,43] and improved methods to mitigate these shifts will improve the metrological characteristics of quantum devices utilizing CPT such as accuracy and long-term stability.[17]

## SUPPLEMENTARY MATERIAL

See supplementary material for details on the four-level density matrix equations, Lorentzian fits to CPT resonances (Fig. 2(a,b)), and calculations of PM light shift suppression scheme limitations.

## ACKNOWLEDGMENTS

We thank Aly Artusio-Glimpse and Isaac Fan for thoughtful comments on this work. This work was performed under the following financial assistance award 70NANB18H006 from U.S. Department of Commerce, National Institute of Standards and Technology. V.I.Y., M.Y.B., and D.V.K. were supported by the Russian Science Foundation (#21-12-00057). V.I.Y. was also supported by the Russian Foundation for Basic Research (#20-02-00505), Ministry of Education and Science of the Russian Federation (#FSUS-2020-0036) and Foundation for the Advancement of Theoretical Physics and Mathematics "BASIS".

## DATA AVAILABILITY STATEMENT

Data are available from the corresponding author upon reasonable request.

[1] L. Maleki and J. Prestage, Metrologia **42**, S145 (2005).
[2] F. Riehle, *Frequency Standards: Basics and Applications* (John Wiley & Sons, 2006).
[3] J. D. Prestage and G. L. Weaver, Proceedings of the IEEE **95**, 2235 (2007).
[4] A. Derevianko and M. Pospelov, Nat. Phys. **10**, 933 (2014).
[5] J. Vanier and C. Tomescu, *The Quantum Physics of Atomic Frequency Standards: Recent Developments* (CRC Press, 2015).
[6] C. Lisdat, G. Grosche, N. Quintin, C. Shi, S. M. F. Raupach, C. Grebing, D. Nicolodi, F. Stefani, A. Al-Masoudi, S. Dörscher, S. Häfner, J.-L. Robyr, N. Chiodo, S. Bilicki, E. Bookjans, A. Koczwara, S. Koke, A. Kuhl, F. Wiotte, F. Meynadier, E. Camisard, M. Abgrall, M. Lours, T. Legero, H. Schnatz, U. Sterr, H. Denker, C. Chardonnet, Y. Le Coq, G. Santarelli, A. Amy-Klein, R. Le Targat, J. Lodewyck, O. Lopez, and P.-E. Pottie, Nat. Commun. **7**, 12443 (2016).
[7] Y. Bock and D. Melgar, Rep. Prog. Phys. **79**, 106801 (2016).
[8] T. E. Mehlstäubler, G. Grosche, C. Lisdat, P. O. Schmidt, and H. Denker, Rep. Prog. Phys. **81**, 064401 (2018).
[9] M. S. Safronova, Ann. Phys. **531**, 1800364 (2019).

[10]G. Alzetta, A. Gozzini, L. Moi, and G. Orriols, Il Nuovo Cimento B **36**, 5 (1976).
[11]B. D. Agap'ev, M. B. Gornyĭ, B. G. Matisov, and Yu V. Rozhdestvenskiĭ, Phys.-Uspekhi **36**, 763 (1993).
[12]E. Arimondo, *Progress in Optics*, Vol. 35 (Elsevier, 1996) Chap. 5, pp. 257–354.
[13]J. Vanier, Appl. Phys. B **81**, 421 (2005).
[14]V. Shah and J. Kitching (Academic Press, 2010) pp. 21–74.
[15]S. Knappe, P. D. D. Schwindt, V. Shah, L. Hollberg, J. Kitching, L. Liew, and J. Moreland, Opt. Express **13**, 1249 (2005).
[16]Z. Wang, Chin. Phys. B **23**, 030601 (2014).
[17]J. Kitching, Appl. Phys. Rev. **5**, 031302 (2018).
[18]M. Zhu and L. S. Cutler, in *Proceedings of the 32th Annual Precise Time and Time Interval Systems and Applications Meeting* (2000) pp. 311–324.
[19]V. Gerginov, S. Knappe, V. Shah, P. D. D. Schwindt, L. Hollberg, and J. Kitching, J. Opt. Soc. Am. B **23**, 593 (2006).
[20]N. Castagna, R. Boudot, S. Guérandel, E. de Clercq, N. Dimarcq, and A. Clairon, IEEE Transactions on Ultrasonics, Ferroelectrics, and Frequency Control **56**, 246 (2009).
[21]D. Miletic, C. Affolderbach, M. Hasegawa, R. Boudot, C. Gorecki, and G. Mileti, Appl. Phys. B **109**, 89 (2012).
[22]D. S. Chuchelov, V. V. Vassiliev, M. I. Vaskovskaya, V. L. Velichansky, E. A. Tsygankov, S. A. Zibrov, S. V. Petropavlovsky, and V. P. Yakovlev, Phys. Scr. **93**, 114002 (2018).
[23]C. Carlé, M. Petersen, N. Passilly, M. A. Hafiz, E. de Clercq, and R. Boudot, IEEE Transactions on Ultrasonics, Ferroelectrics, and Frequency Control **68**, 3249 (2021).
[24]P. R. Hemmer, M. S. Shahriar, V. D. Natoli, and S. Ezekiel, J. Opt. Soc. Am. B **6**, 1519 (1989).
[25]Y. Yano, W. Gao, S. Goka, and M. Kajita, Phys. Rev. A **90**, 013826 (2014).
[26]G. S. Pati, Z. Warren, N. Yu, and M. S. Shahriar, J. Opt. Soc. Am. B **32**, 388 (2015).
[27]M. Abdel Hafiz, G. Coget, P. Yun, S. Guérandel, E. de Clercq, and R. Boudot, J. Appl. Phys. **121**, 104903 (2017).
[28]X. Liu, E. Ivanov, V. I. Yudin, J. Kitching, and E. A. Donley, Phys. Rev. Appl. **8**, 054001 (2017).
[29]J. W. Pollock, V. I. Yudin, M. Shuker, M. Yu. Basalaev, A. V. Taichenachev, X. Liu, J. Kitching, and E. A. Donley, Phys. Rev. A **98**, 053424 (2018).
[30]V. Shah, V. Gerginov, P. Schwindt, S. Knappe, L. Hollberg, and J. Kitching, Appl. Phys. Lett. **89**, 151124 (2006).
[31]M. I. Vaskovskaya, E. A. Tsygankov, D. S. Chuchelov, S. A. Zibrov, V. V. Vassiliev, and V. L. Velichansky, Opt. Express **27**, 35856 (2019).
[32]S. Yanagimachi, K. Harasaka, R. Suzuki, M. Suzuki, and S. Goka, Appl. Phys. Lett. **116**, 104102 (2020).
[33]M. Yu. Basalaev, V. I. Yudin, A. V. Taichenachev, M. Vaskovskaya, D. S. Chuchelov, S. A. Zibrov, V. V. Vassiliev, and V. L. Velichansky, Phys. Rev. Appl. **13**, 034060 (2020).
[34]C. Sanner, N. Huntemann, R. Lange, C. Tamm, and E. Peik, Phys. Rev. Lett. **120**, 053602 (2018).
[35]V. I. Yudin, A. V. Taichenachev, M. Yu. Basalaev, T. Zanon-Willette, J. W. Pollock, M. Shuker, E. A. Donley, and J. Kitching, Phys. Rev. Appl. **9**, 054034 (2018).
[36]V. I. Yudin, A. V. Taichenachev, M. Y. Basalaev, T. Zanon-Willette, T. E. Mehlstäubler, R. Boudot, J. W. Pollock, M. Shuker, E. A. Donley, and J. Kitching, New J. Phys. **20**, 123016 (2018).
[37]M. Abdel Hafiz, G. Coget, M. Petersen, C. Rocher, S. Guérandel, T. Zanon-Willette, E. de Clercq, and R. Boudot, Phys. Rev. Appl. **9**, 064002 (2018).
[38]M. Abdel Hafiz, G. Coget, M. Petersen, C. Calosso, S. Guérandel, E. de Clercq, and R. Boudot, Appl. Phys. Lett. **112**, 244102 (2018).
[39]M. Shuker, J. W. Pollock, R. Boudot, V. I. Yudin, A. V. Taichenachev, J. Kitching, and E. A. Donley, Phys. Rev. Lett. **122**, 113601 (2019).
[40]M. Shuker, J. W. Pollock, R. Boudot, V. I. Yudin, A. V. Taichenachev, J. Kitching, and E. A. Donley, Appl. Phys. Lett. **114**, 141106 (2019).
[41]M. Yu. Basalaev, V. I. Yudin, D. V. Kovalenko, T. Zanon-Willette, and A. V. Taichenachev, Phys. Rev. A **102**, 013511 (2020).
[42]V. I. Yudin, M. Y. Basalaev, A. V. Taichenachev, J. W. Pollock, Z. L. Newman, M. Shuker, A. Hansen, M. T. Hummon, R. Boudot, E. A. Donley, and J. Kitching, Phys. Rev. Appl. **14**, 024001 (2020).
[43]M. Abdel Hafiz, R. Vicarini, N. Passilly, C. E. Calosso, V. Maurice, J. W. Pollock, A. V. Taichenachev, V. I. Yudin, J. Kitching, and R. Boudot, Phys. Rev. Appl. **14**, 034015 (2020).
[44]A. Nagel, S. Brandt, D. Meschede, and R. Wynands, Euro. Phys. Lett. **48**, 385 (1999).
[45]E. E. Mikhailov, T. Horrom, N. Belcher, and I. Novikova, J. Opt. Soc. Am. B **27**, 417 (2010).
[46]S. A. Zibrov, I. Novikova, D. F. Phillips, R. L. Walsworth, A. S. Zibrov, V. L. Velichansky, A. V. Taichenachev, and V. I. Yudin, Phys. Rev. A **81**, 013833 (2010).
[47]R. Boudot, P. Dziuban, M. Hasegawa, R. K. Chutani, S. Galliou, V. Giordano, and C. Gorecki, J. Appl. Phys. **109**, 014912 (2011).
[48]J. C. Camparo, R. P. Frueholz, and C. H. Volk, Phys. Rev. A **27**, 1914 (1983).
[49]J. C. Camparo, Phys. Rev. A **39**, 69 (1989).
[50]F. Levi, A. Godone, J. Vanier, S. Micalizio, and G. Modugno, Eur. Phys. J. D **12**, 53 (2000).
[51]H. Gilles, B. Cheron, O. Emile, F. Bretenaker, and A. Le Floch, Phys. Rev. Lett. **86**, 1175 (2001).
[52]A. V. Taichenachev, A. M. Tumaikin, V. I. Yudin, M. Stähler, R. Wynands, J. Kitching, and L. Hollberg, Phys. Rev. A **69**, 024501 (2004).
[53]M. Radonjić, D. Arsenović, Z. Grujić, and B. M. Jelenković, Phys. Rev. A **79**, 023805 (2009).
[54]I. Novikova, Y. Xiao, D. F. Phillips, and R. L. Walsworth, J. Mod. Opt. **52**, 2381 (2005).
[55]Y. Xiao, I. Novikova, D. F. Phillips, and R. L. Walsworth, Phys. Rev. Lett. **96**, 043601 (2006).
[56]Y. Xiao, I. Novikova, D. F. Phillips, and R. L. Walsworth, Opt. Express **16**, 14128 (2008).
[57]J. Vanier, M. W. Levine, D. Janssen, and M. Delaney, Phys. Rev. A **67**, 065801 (2003).
[58]G. A. Pitz, A. J. Sandoval, T. B. Tafoya, W. L. Klennert, and D. A. Hostutler, J. Quant. Spectrosc. Radiat. Transf. **140**, 18 (2014).
[59]V. I. Yudin, M. Yu. Basalaev, D. V. Kovalenko, A. V. Taichenachev, J. W. Pollock, A. Hansen, W. R. McGehee, and J. Kitching, Quantum Electron. **52** (2020).
[60]J. Berberian, L. Cutler, and M. Zhu, in *Proceedings of the 2004 IEEE International Frequency Control Symposium and Exposition, 2004.* (IEEE, 2004) pp. 137–143.
[61]A. V. Taichenachev, V. I. Yudin, R. Wynands, M. Stähler, J. Kitching, and L. Hollberg, Phys. Rev. A **67**, 033810 (2003).